Eur. Phys. J. D **54**, 445–449 (2009)
DOI: 10.1140/epjd/e2009-00004-2

THE EUROPEAN PHYSICAL JOURNAL D

Regular Article

Influence of the surface conditions on rf plasma characteristics

M. Radmilović-Radjenović[a] and Z.Lj. Petrović

Institute of Physics, Pregrevica 118, 11080 Belgrade, Serbia

Received 3rd September 2008 / Received in final form 5 December 2008
Published online 16 January 2009 –

Abstract. The secondary electron emission is a surface dependent phenomenon, more influenced by surface preparation than by the material itself. The present paper deals with the effect of the electrode surface conditions: clean (atomically clean) and contaminated electrodes (standard conditions even after mechanical and chemicals cleaning) on the characteristics of an asymmetric discharge by PIC/MCC simulations. In the arrangement with one clean and one contaminated electrode the discharge characteristics strongly depend upon which electrode is powered. The obtained PIC/MCC simulation results indicate that contamination of electrodes and variations of the secondary electron emission coefficients can lead to more or less significant changes in properties of rf plasmas.

PACS. 79.20.Rf Atomic, molecular, and ion beam impact and interactions with surfaces – 79.20.Ap Theory of impact phenomena; numerical simulation

1 Introduction

Bombardment of the substrate surface by energetic ions represents a basic physical process that occurs in capacitively couples plasma (CCP) sources making them very useful as plasma processing devices [1–4]. Electron emission from solids under ion bombardment may give a significant contribution to overall electron production and it has been subject of numerous investigations [5–10] due to its relevance for many applications like electrical discharges [11–13], plasma-wall interaction [14], single-particle detection [15,16] and studies of breakdown [17–19]. More recently, particle-induced electron emission has attracted a renewed interest due to its key role in plasma display panels, where it affects firing and sustaining voltage and therefore the power consumption of the panels [20–22], for spacecraft charging as the cause of many system anomalies and component failures [23] and for determination of the scaling laws in microdischarges [24–26].

Secondary electron emission is commonly ascribed to two different mechanisms, the potential emission and the kinetic emission processes. At very low kinetic ion energy, the emission process is determined by the ionization energy of the ion the so called the potential electron emission which is found to be very sensitive to surface contamination. Above a certain threshold, typically of the order of a few hundred electronvolts, the kinetic ion energy dominates the emission process (kinetic electron emission) [27].

Secondary emission coefficients may vary significantly depending on the surface conditions and flux of species arriving to the surface [28]. The origin of the differences in the values of the secondary electron yields between clean materials and dirty (known also as a technical) materials is due to the presence of a surface layer (oxide and contaminants). An overall review of secondary electron emission data for various electrode materials, especially significant in plasma modelling, can be found in [29]. In the present paper, the influence of the electrode conditions (clean and contaminated electrodes) on characteristics of the asymmetric discharge has been studied by means of particle-in-cell/Monte Carlo collision (PIC/MCC) simulations.

2 Simulation technique

The simulation code used in this work is one-dimensional electrostatic particle-in-cell (PIC) code with Monte-Carlo collision model (MCC) [30,31]. In PIC simulations, the so-called "superparticles" move in the discharge space through an artificial spatial grid through time steps. Only charged particles are simulated. Initially, superparticles are distributed in the simulation domain and a self-consistent potential distribution is determined based on the positions of superparticles and externally applied voltage. The particle equations of motion are advanced one time step, using fields interpolated from the discrete grid to the continuous particles locations. Source terms and parameters for the field equations are accumulated from the continuous particle locations to the discrete mesh locations. The fields are then advanced in time. If the system is collisional, the Monte Carlo collision scheme is applied [32]. Choices of boundary conditions depend on

[a] e-mail: marija@phy.bg.ac.yu

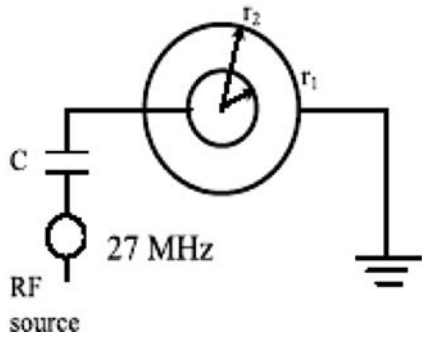

Fig. 1. Schematic diagram of the CCP source with cylindrical electrodes leading to an asymmetric system (in our case the electrode area ratio was 1.73).

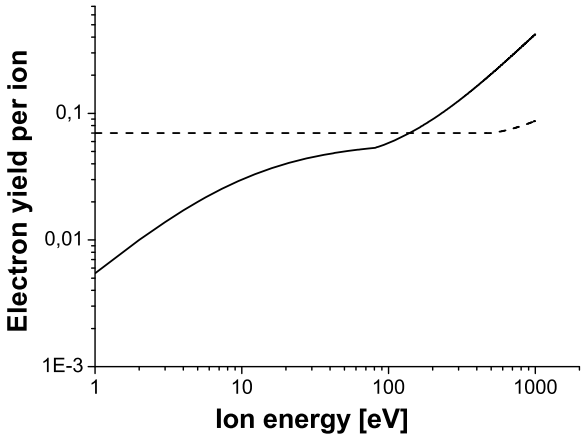

Fig. 2. Dependence of the electron yield on the ion energy when Ar^+ ions incident on clean (dashed line) and dirty (solid) surfaces [29].

the physical conditions of the boundary walls and electrodes. When an electron reaches the boundary, it is assumed to be absorbed. On the other hand, when an ion hits the surface, secondary electron may be emitted with a probability depending on the impinging ion energy. The PIC/MCC method represents a self-consistent and fully kinetic approach capable of predicting energy distribution function (EEDF) with strict kinetic treatment of electrons in spatially inhomogeneous plasma and ion energy distribution function (IEDF) for ions arriving at the electrodes.

In this paper, we have performed PIC/MCC simulations of one-dimensional cylindrical geometry model shown in Figure 1. Electrodes are made of the same material but with different secondary electron emission coefficients due to different surface conditions (as described in [29]). The inner electrode is capacitively coupled to the rf source at 27 MHz, while the outer electrode is grounded. The discharge is maintained between these two electrodes separated by a gap of 2 cm. We trace the argon plasma parameters along the r-axis. In order to obtain the meaningful results, we performed the simulation runs for several thousand rf cycles. In this study, the term RHS electrode is related to the large electrode, while the small electrode is referred to as the LHS electrode [33]. It was shown that the sufficient number of superparticles represents one of the critical conditions for the reliability of the PIC/MCC simulations [34,35]. The accuracy is limited by the statistical fluctuations if we assume that the model is exact. Thus statistical uncertainty may be seen from the fluctuations of the data. To reduce the statistical noise, that is inversely proportional to the number of superparticles, the total number of the superparticles for electrons (or ions) at the steady state was made to be approximately 10^5.

2.1 Ion induced secondary electron emission

In general, the secondary electron emission consists of three elementary steps: (1) release of electrons inside a solid as a result of collisions with incident particles; (2) transport to surface of the released electrons and (3) escape from the surface [36]. Numerous publications have been devoted to the details of the release of electrons from surfaces [36] and to electron emission efficiencies due to bombardment of different surfaces (for example of the so-called clean and dirty surfaces as defined in [29] and references in it) by positive rare gas ions.

The secondary electron emission from a surface under the action of an ion is represented by the the electron yield per ion γ_i quantifying the effective number (probability) of electrons leaving the surface of the instantaneous cathode per one impinging ion. Although, the yield of secondary electrons depends on the ion species, their energy, the target material and the gas it was often assumed to be constant [37–39] causing discrepancies between experimental and simulation results for plasma characteristics. In order to correct this deficiency, Phelps and co-workers have suggested the energy dependence of the effective yields for clean and dirty surfaces, respectively [29,40]:

$$\gamma_i^c = 0.07 + \frac{1 \times 10^{-5}(\varepsilon_i - 500)^{1.2}}{1 + (\varepsilon_i/70000)^{0.7}}, \quad (1)$$

$$\gamma_i^d = \frac{0.006\varepsilon_i}{1 + (\varepsilon_i/10)} + \frac{1.05 \times 10^{-4}(\varepsilon_i - 80)^{1.2}}{[1 + (\varepsilon_i/8000)]^{1.5}}, \quad (2)$$

where the contribution of the second term is zero for the incident ion energy ε_i below 500 eV and 80 eV, respectively. Figure 2 illustrates the difference between the solid curve that shows fits to the experimental beam data for 'dirty' surfaces and the dashed curve that corresponds to the yield for clean surfaces. By 'dirty' these authors mean that the surfaces were prepared by taking the standard mechanical and chemical cleaning procedures while by clean they imply that the surfaces are atomically clean which may be achieved only by heating or ion bombardment in vacuum and thereby is impossible to achieve in standard gas discharges [29].

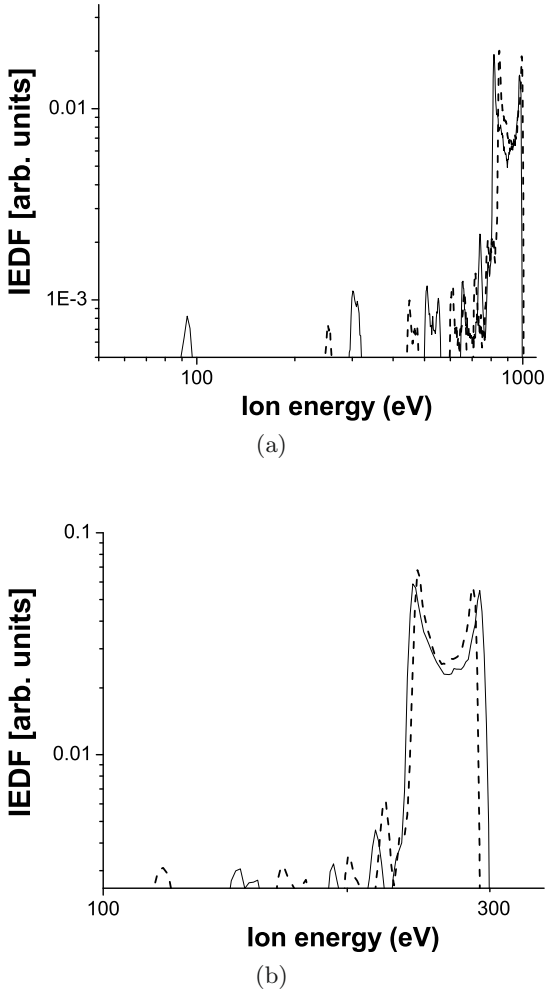

Fig. 3. IEDF for Ar^+ ions arriving to: (a) LHS (small) and (b) RHS (large) electrode. Solid line corresponds to the arrangement when small (powered) electrode is contaminated and the large one is clean. Dashed line represents the case when small electrode is clean and the large one is contaminated.

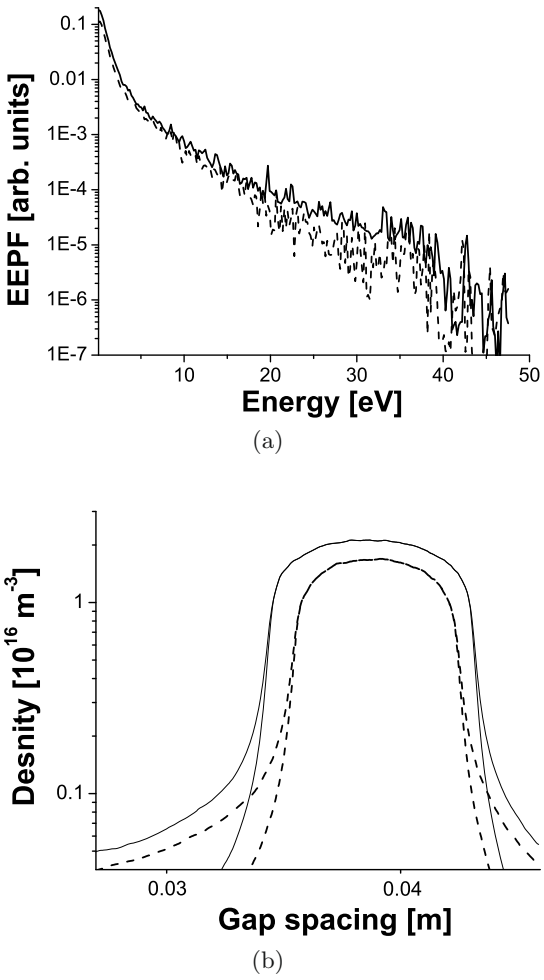

Fig. 4. Effect of electrode surface conditions on (a) electron energy probability function and (b) density profile. The definition of lines is the same as in Figure 3.

3 Results

Due to discharge asymmetry (see Fig. 1), ions with different energies collide with the powered and grounded electrodes. In the configuration with one clean and one contaminated electrode the discharge characteristics depend upon which electrode is powered. Figure 3 shows that a significant difference in the IEDF is noticed in the case of contaminated powered – clean grounded electrodes (solid lines) (see Fig. 3a) as compared to those when electrode conditions are changed (see Fig. 3b). The maximum applied voltages were 1000 V for the data in Figure 3a and 300 V for the case depicted in Figure 3b. The power was low in the limit of low powers but it could not be defined very well for the geometry of our system.

As a result bulk properties of the plasma are different (as shown in Fig. 4) although, electron energy probability function (EEPF) is not very sensitive to the surface conditions as presented in Figure 4a with differences only occurring at higher energies.

Energetic secondaries can ionize the background gas leading to an increase of the plasma density, that is substantially higher under circumstance with contaminated powered – clean grounded electrodes (solid line) as can be observed from Figure 4b. As a consequence of the discharge asymmetry, for different discharge configurations, fluxes of Ar^+ ions arriving to the powered electrode are also different under different conditions of electrodes, which is presented in Figure 5. On the other hand, Figure 6 clearly demonstrates that surface conditions of the electrodes have a minor effect on plasma potential which is slightly higher when small electrode is contaminated.

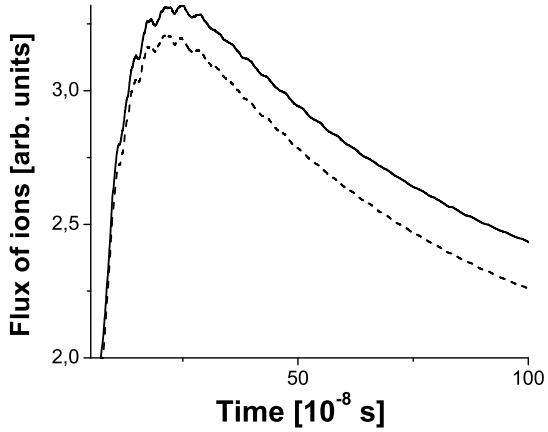

Fig. 5. Time dependence of the flux of Ar^+ ions arriving at the large electrode. The definition of lines is the same as in Figure 3.

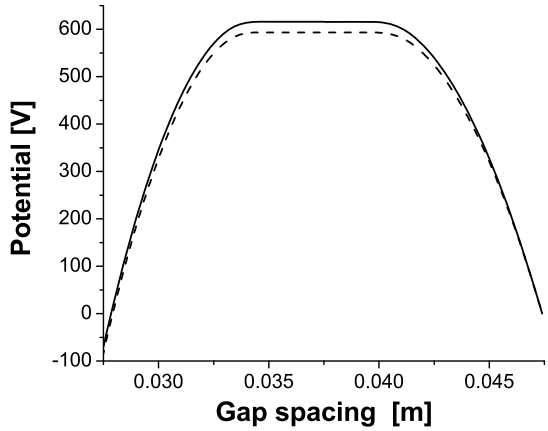

Fig. 6. Time averaged potential profile for contaminated powered – clean grounded electrodes (solid line) and clean powered – contaminated grounded electrodes (dashed line).

4 Conclusions

Depending on the characteristics of the incident ions and on the surface conditions, secondary emission of electrons and ions may be affected in various ways. In asymmetric discharge with different treatment of the electrode surfaces, the electron yield per ion is different for small and large electrodes leading to different energy of ions bombarding the powered and grounded electrodes. Due to contamination, the electron yield for the powered electrode can be an order of magnitude larger. On average, the secondary electron yield is larger for dirty surfaces and for ion energies as observed in the discharge, although secondary emission coefficients may fluctuate remarkably not only with changing of the surface conditions but also with variation of the flux of species arriving at the surface.

In this paper, the PIC/MCC code has been applied in order to study the effect of the secondary electron emission on rf plasma characteristics. We have employed clean and dirty metal surfaces, based on literature data [29]. In our simulations we have implemented a more accurate model of the secondary electron production per ion suggested by Phelps and Petrović, that includes the energy dependence of the yield. While one could argue that the choice of conditions may not be appropriate it is quite likely that heavy ion bombardment by at high energies may lead to what was labelled as 'clean' conditions in [29]. On the other hand different characteristics of ions falling on the surfaces of two electrodes in an asymmetric system may induce similar differences in the properties as assumed here. The same or even greater differences may be caused by deposition of sputtered material or chemically modified surfaces due to the presence or reactive species. Most of all presence of wafer on one of the two electrodes especially when silicone dioxide is etched will result in very large differences in secondary electron yields at the two electrodes.

Results of simulations confirm that plasma characteristics are more or less sensitive to the secondary yields from the powered electrode. The ion energy distribution functions, plasma density and flux of ions arriving at the grounded electrode greatly respond to the surface conditions of the powered electrode. On the other hand, the electron energy probability function and time average potential profile are not so significantly influenced by the surface preparation. The effects discussed here will become more important as power deposited to the plasma increases.

The present work has been performed under MNZŽS 141025 project.

References

1. V.A. Godyak, R.B. Piejak, B.M. Alexandrovich, J. Appl. Phys. **69**, 3455 (1991)
2. M.A. Lieberman, A.J. Lichtenberg, *Principles of Plasmas Discharges and Material Processing* (Wiley, New York, 1994)
3. T. Makabe, Z.Lj. Petrović, *Advances in Low Temperature RF Plasmas* (Elsevier, New York, 2002)
4. T. Makabe, Z.Lj. Petrović, *Plasma Electronics: Applications in Microelectronic Device Fabrication* (Taylor & Francis, 2006)
5. J.P. Molnar, Phys. Rev. **83**, 940 (1951)
6. P.H. Mahadevan, J.K. Layton, D.B. Medvedev, Phys. Rev. **129**, 79 (1963)
7. P.H. Mahadevan, G.D. Magnuson, J.K. Layton, C.E. Carlston, Phys. Rev. **140**, A1407 (1965)
8. G. Holmen, B. Svensson, J. Schou, P. Sigmund, Phys. Rev. B **20**, 2247 (1979)
9. A. Itoh, T. Majima, F. Obata, Y. Hamamoto, A. Yogo, Nucl. Instrum. Meth. B **192**, 626 (2002)
10. A. Bogaerts, R. Gijbels, Plasma Sources Sci. Technol. **11**, 27 (2002)
11. S. Kakuta, F. Tochikubo, Z.Lj. Petrović, T. Makabe, J. Appl. Phys. **74**, 4923 (1993)

12. R. Krimke, H.M. Urbassek, J. Phys. D **29**, 378 (1996)
13. D. Marić, K. Kutasi, G. Malović, Z. Donk, Z.Lj. Petrović, Eur. Phys. J. D **21**, 73 (2002)
14. L. Jolivet, J.F. Roussel, IEEE Trans. Plasma Sci. **30**, 318 (2001)
15. S.F. Biagi, D. Duxbury, E. Gabathuler, Nucl. Instrum. Meth. A **419**, 438 (1998)
16. A. DiMauro, E. Nappi, F. Posa, A. Breskin, A. Ozulutskov, R. Chechik, S.F. Biagi, G. Paic, F. Piuz, Nucl. Instrum. Meth. A **371**, 137 (1996)
17. V.Lj. Marković, S.R. Gocić, S.N. Stamenković, Z.Lj. Petrović, M. Radmilović, Eur. Phys. J. Appl. Phys. **4**, 171 (2001)
18. D. Mariotti, J.A. McLaughlin, P. Maguire, Plasma Sources Sci. Technol. **13**, 207 (2004)
19. M. Radmilović-Radjenović, J.K. Lee, Phys. Plasmas **15**, (2005)
20. C. Punset, J.P. Boeuf, L.C. Pitchford, J. Appl. Phys. **83**, 1884 (1998)
21. V.P. Nagorny, P.J. Drallos, W. Williamson, Jr, J. Appl. Phys. **77**, 3645 (1995)
22. S.S. Yang, S.M. Lee, F. Iza, J.K. Lee, J. Phys. D: Appl. Phys. **39**, 2775 (2006)
23. T.B. Frooninckx, J.J. Sojka, J. Geophys. Res. **97**, 2985 (1992)
24. M. Radmilović-Radjenović, J.K. Lee, F. Iza, G.Y. Park, J. Phys. D **38**, 950 (2005)
25. M. Radmilović-Radjenović, B. Radjenović, Plasma Sources Sci. Technol. **16**, 337 (2007)
26. M. Radmilović-Radjenović, B. Radjenović, Contrib. Plasma Phys. **47**, 165 (2007)
27. A. Qayyum, I. Mehmood, W. Ahmad, The Nucleus **41**, 1 (2004)
28. E.V. Barnat, G.A. Hebener, J. Appl. Phys. **98**, 013305 (2005)
29. A.V. Phelps, Z.Lj. Petrović, Plasma Sources Sci. Technol. **8**, R21 (1999)
30. C.K. Birdsall, IEEE Trans. Plasma Sci. **19**, 65 (11991)
31. J.P. Verboncoeur, M.V. Alves, V. Vahedi, C.K. Birdsall, J. Comput. Phys. **104**, 321 (1993)
32. V. Vahedi, M. Surendra, Comput. Phys. Commun. **87**, 179 (1995)
33. N.Yu Babaeva, J.K. Lee, J.W. Shon, J. Phys. D: Appl. Phys. **38**, 287 (2005)
34. I.V. Schweigert, V.A. Schweigert, Plasma Sources Sci. Technol. **13**, 315 (2004)
35. H.C. Kim, O. Manuilenko, J.K. Lee, Jpn J. Appl. Phys. **44**, 1957 (2005)
36. E.J. Sternglass, Phys. Rev. **108**, 1 (1957)
37. J.P. Boeuf, Phys. Rev. A **36**, 2782 (1987)
38. M. Soji, M. Sato, J. Phys. D: Appl. Phys. **32**, 1640 (1999)
39. H.B. Smith et al., Phys. Plasmas **10**, 875 (2003)
40. A.V. Phelps, L.C. Pitchford, C. Pedoussat, Z. Donko, Plasma. Sources Sci. Technol. **8**, B1 (1999)